DE GRUYTER OPEN

Acta Geophysica
vol. 64, no. 1, Feb. 2016, pp. 76-100
DOI: 10.1515/acgeo-2015-0060

Shear Wave Splitting Analysis to Estimate Fracture Orientation and Frequency Dependent Anisotropy

Raoof GHOLAMI[1], Ali MORADZADEH[1,2], Vamegh RASOULI[3], and Javid HANACHI[4]

[1]Department of Chemical and Petroleum Engineering, Curtin University, Sarawak, Malaysia; e-mail: Raoof.Gholami@Curtin.edu.my

[2]Department of Mining, Petroleum and Geophysics, Shahrood University of Technology, Shahrood, Iran

[3]Department of Petroleum Engineering, University of North Dakota, Grand Forks, USA

[4]Petroleum Geology, Tehran, Iran

Abstract

Shear wave splitting is a well-known method for indication of orientation, radius, and length of fractures in subsurface layers. In this paper, a three component near offset VSP data acquired from a fractured sandstone reservoir in southern part of Iran was used to analyse shear wave splitting and frequency-dependent anisotropy assessment. Polarization angle obtained by performing rotation on radial and transverse components of VSP data was used to determine the direction of polarization of fast shear wave which corresponds to direction of fractures. It was shown that correct implementation of shear wave splitting analysis can be used for determination of fracture direction. During frequency-dependent anisotropy analysis, it was found that the time delays in shear-waves decrease as the frequency increases. It was clearly demonstrated throughout this study that anisotropy may have an inverse relationship with frequency. The analysis presented in this paper complements the studied conducted by other researchers in this field of research.

Key words: shear wave splitting, Vertical Seismic Profile, fracture, frequency dependent anisotropy, southern part of Iran.

1. INTRODUCTION

Fractures are geological features in the subsurface layers controlling mechanical strength and transport properties of different formations. Fracture systems are also key parameters for hydrocarbon production, manipulation of water supplies as well as dispersion of pollutants into aquifer. Fractures are usually considered to be one of the dominant causes of observing anisotropy in hydrocarbon reservoirs.

Most of our understanding about the subsurface layers is coming from seismic data analysis. The unique properties of *S*-waves can provide significant added value over conventional *P*-wave methods. For example, *S*-wave velocity contrast of sand channels has recently been found to be a perfect asset in delineating the limits and morphology of the Alba field in the North Sea (MacLeod *et al.* 1999). Additionally, the insensitivity of *S*-waves to pore fluids has been revealed to be a great help in imaging the structure of the Valhall where *P*-wave structural could not be very helpful due to presence of a gas chimney (Thomsen *et al.* 1997). One of the most successful methods in characterization of fractures behavior is also shear waves' data analysis (Crampin 1985). As a matter of fact, one commonly used method to examine fracture-induced azimuthal anisotropy is shear-wave splitting analysis. In this type of analysis, strike of fractures is derived from polarization direction of fast shear-waves and fracture density can be given by time delay between the fast and slow shear-waves.

In the last decade, it has been found and repeatedly indicated that splitting of shear-waves depends mostly on frequency (Marson-Pidgeon and Savage 1997, Chesnokov *et al.* 2001, Liu *et al.* 2000). Generally speaking, the larger the size of the fractures, the lower the frequency range where velocity dispersion and frequency dependence of anisotropy occur. If multiple fracture sets with different scales are present, say, micro-cracks are aligned in whatever direction from aligned fractures, low frequency would be expected to give the orientation of fractures and high frequency would give the direction of micro-cracks. This may appear initially to be surprising, but we can see later that this can be physically explained. The effect has been observed in VSP data (Chesnokov *et al.* 2001, Liu *et al.* 2003) and used to invert for fracture size. It is also consistent with observations from earthquake data (Marson-Pidgeon and Savage 1997, Liu *et al.* 2000). There is also evidence from measurements taken from a range of experiments that shear wave splitting exhibits frequency dependence (Lynn *et al.* 1999). However, to do frequency dependent anisotropy analysis, there has to be models relating polarization and time delays of split shear-waves to fracture density and orientations. Plenty of these models and theories have been introduced and provided the foundation of anisotropy analysis. However, most theories fail

to provide an adequate explanation of velocity dispersion at seismic frequency and hence variation of anisotropy with frequency is not predicted (Thomsen 1995, Hudson *et al.* 1996, 2001; Hudson 1981, Bayuk and Chesnokov 1998, Chesnokov *et al.* 1998, Liu *et al.* 2000, Pointer *et al.* 2000). Thus, in plenty of cases, scattering of seismic waves and fluid flow are considered as the two mechanisms relating velocity dispersion to fractured rock. Wave scattering mechanism has been studied by Werner and Shapiro (1999) and Chesnokov *et al.* (2001) whereas fluid flow has been evaluated by Magnitsky and Chesnokov (1986), Bayuk and Chesnokov (1998), Parra (2000), and Tod and Liu (2002). Among these, Bayuk and Chesnokov (1998), Chapman *et al.* (2003), and Tod and Liu (2002) presented theoretical models to evaluate vertically aligned fractures in porous rocks. Lynn *et al.* (1995, 1996, 1999) also used *P*- and *S*-wave azimuthal anisotropy to characterize fractured reservoirs. As a matter of fact, many theoretical and field studies have shown that the azimuthal variation in wavefield attributes (such as velocity and amplitude) can be used for fracture detection (Tsvankin 1997, Li *et al.* 2003, Vetri *et al.* 2003, Zhu *et al.* 2008, Qian *et al.* 2008). However, only a few consider frequency dependencies in physical characteristics of anisotropic media.

In this study, three-component near offset VSP data acquired from a fractured sandstone reservoir in a field located in southern part of Iran was used to evaluate fracture orientation and analyse frequency dependent anisotropy. Techniques used to process the three-component VSP data, shear-waves splitting, and frequency dependent analysis will be presented and discussed in details.

2. GEOLOGICAL SETTING AND AVAILABLE DATA

The study field is located at approximately 90 km distance offshore Kharg Island and was discovered by AGIP in 1966. The field is a NNE-SSW trending, elongated anticline, with dimensions and thickness of approximately 100 km^2 and 250 m, respectively, and is within the Burgan fractured sandstone reservoir. While the fractured reservoir introduces highly anisotropic and shear splitting environment, in this field the cap rock shale formation has resulted in a dominant anisotropic behavior in the subsurface layers. The structure has a pronounced southern culmination and is faulted along its crest. A significant collapse is present over the northern culmination that has a lower structural relief than the southern one. Uncertainty related to the depth of the flanks of the structure exists due to the lack of velocity data. The faults do not extend across the entire structure and reservoir continuity and connectivity is expected to be maintained within the oil column resulting in a field wide common pressure regime. The minor displacement along the faults combined with the high sand content limits the potential for develop-

ment of fault seals. However, uncertainty exists on the sealing potential of individual faults. Some faults may seal and most faults are expected to form partial flow barriers resulting in tortuous flow paths across faults. The geological reports indicate heterogeneity and uncertainties related to the actual location and correlatability of the good quality sands. Matrix porosity and permeability of the reservoir rocks are generally low (porosity is less than 10% and permeability is less than 5 mD); however, natural fractures can assist in higher production rates. Two fracture sets were identified during surface mapping; one is striking N10E and the other is striking N73W to N87W. Maximum horizontal stress direction was estimated as N10E to N20E from borehole elongation observed in four-arm caliper logs in the adjacent wells. The first exploration well, drilled in 1964/65, encountered the Burgan reservoir indicating the structure to be slightly under-filled. Currently, two wells in this field are producing 5000 bbl/d. A total of 15 wells

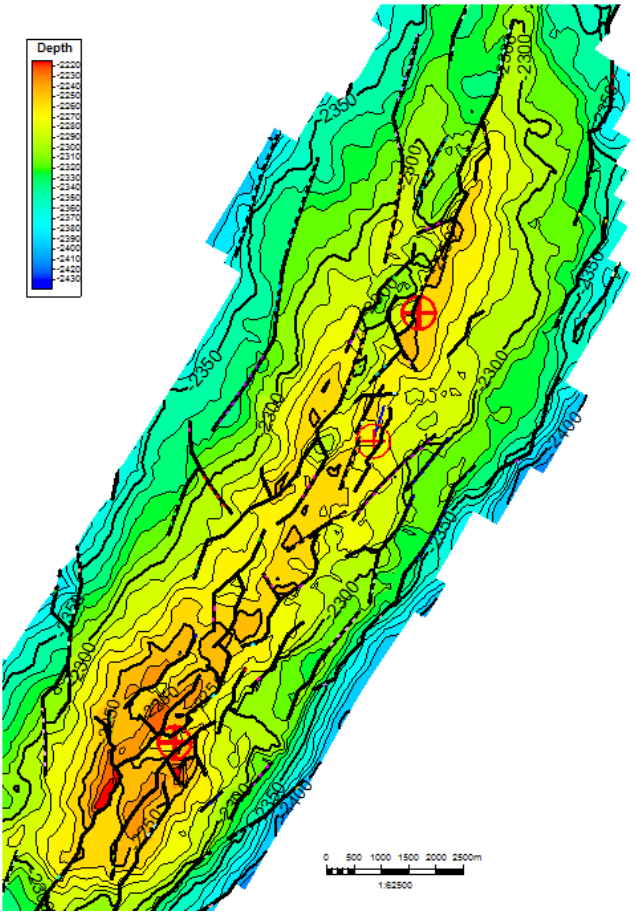

Fig. 1. Geological structure of the Burgan reservoir.

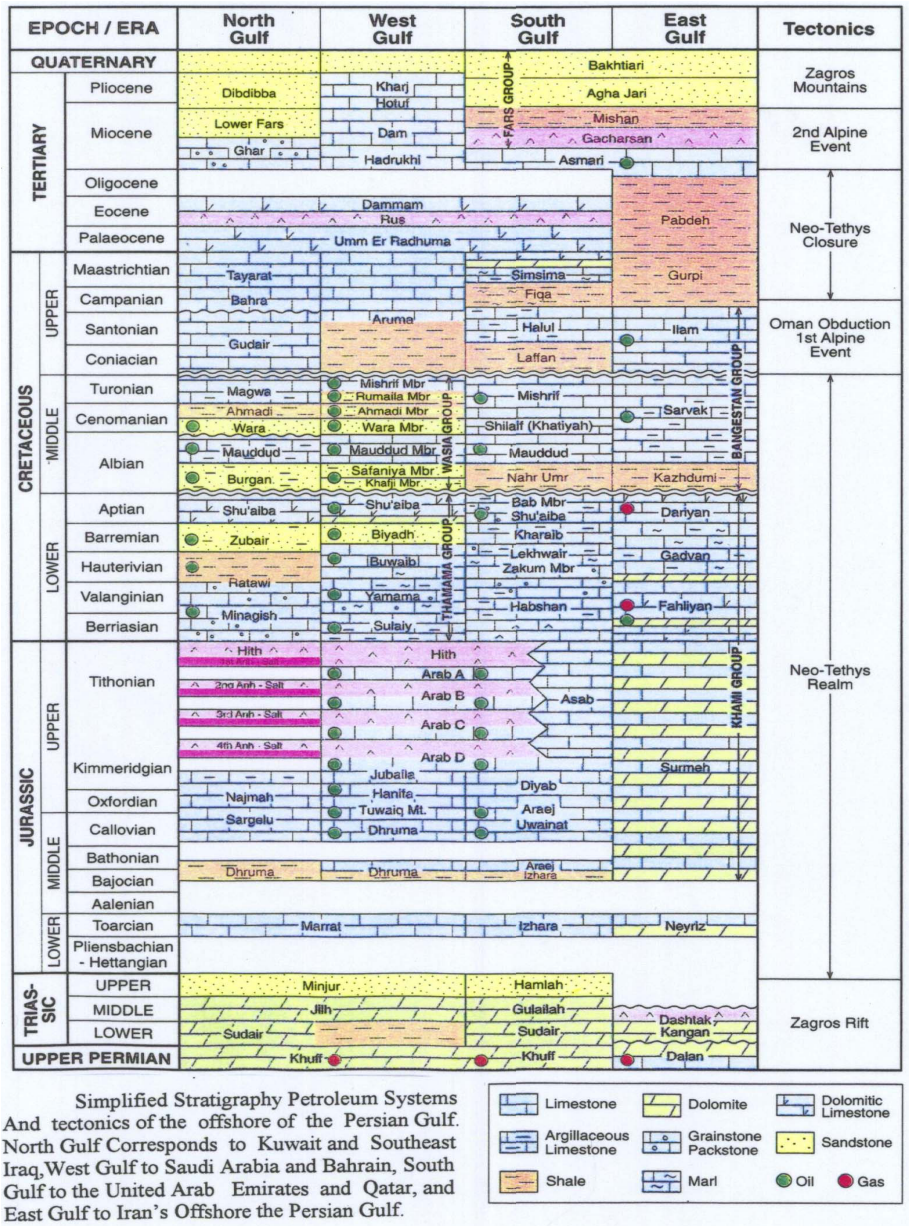

Simplified Stratigraphy Petroleum Systems And tectonics of the offshore of the Persian Gulf. North Gulf Corresponds to Kuwait and Southeast Iraq, West Gulf to Saudi Arabia and Bahrain, South Gulf to the United Arab Emirates and Qatar, and East Gulf to Iran's Offshore the Persian Gulf.

Fig. 2. Geological stratigraphy of the field under study (NISOC 2005).

have been drilled between 1964 and 1970 on the structure. Figure 1 shows the geological structure of the reservoir in this field. Figure 2 shows the geological stratigraphy of the field.

2.1 Offshore well logs, core, and VSP data

In the studied well, a four-armed caliper, multi array sonic log (*i.e.*, shear and compressive waves) together with porosity and density logs and a Vertical Seismic Profile (VSP) were acquired. In addition, to have information about productive zones, two core trips were run to test the acquired cores at later stages. In the study, to obtain information about the properties of the subsurface layers, two core trips were run. In the first run, 23.5 m of the rocks were cored but 21.7 m recovered. In the second run, 16.5 m were cored with 6.5 m being recovered. Visual inspection of the cores showed continuous length of intact rock and some zones that were heavily fractured (see Fig. 3).

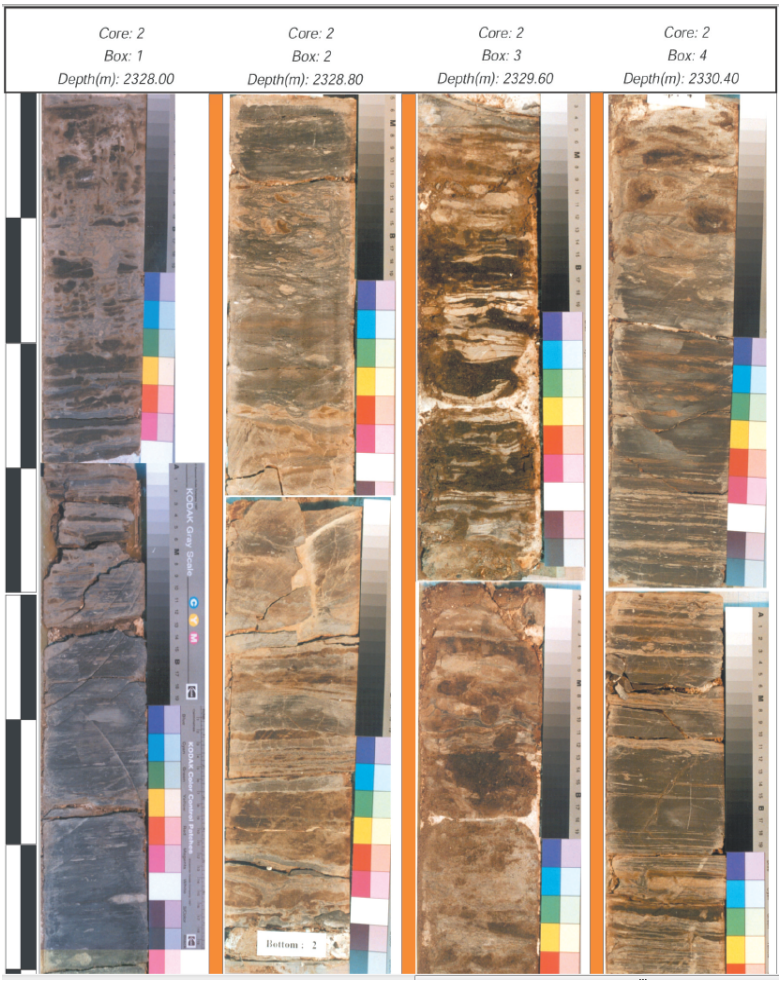

Fig. 3. Fractured core samples obtained from offshore wells (NISOC 2005).

2.2 VSP data acquisition

Due to the topographic relief of the reservoir, accurate positioning of development wells on the structure was particularly important. Thus, a thorough knowledge of the reservoir structure was essential, and the potential of VSP techniques for mapping the reservoir structure was considered to be very critical. In addition, the combined requirements of small size, wide frequency band, directional sensitivity, high data production rate, and relatively low cost were difficult to be met with existing seismic exploration equipment.

The acquisition of the near-offset VSP (*i.e.*, source was located at 50 m distance from well head) was done using an array of two air guns and a three-component downhole geophone. This multi-level three-component receiver chain, with an outside diameter of 43 mm, was designed and built for surveys in deviated boreholes with maximum deviation of around 34 degrees. Two hydrophones were also attached to the source frame. One was used as the time reference and the other as a backup. The acquisition was performed at the depth interval of 60 to 2650 m with a vertical spacing of approximately 15 m between successive geophone stations. The geophone was clamped to the borehole wall at each level but was free to rotate between levels, and the orientation of the horizontal geophone components was not monitored. Data was acquired in different sections of the well from open hole to multiple casing strings at kilometer scale. Figure 4 shows schematically the design and acquisition of VSP data from the well under consideration.

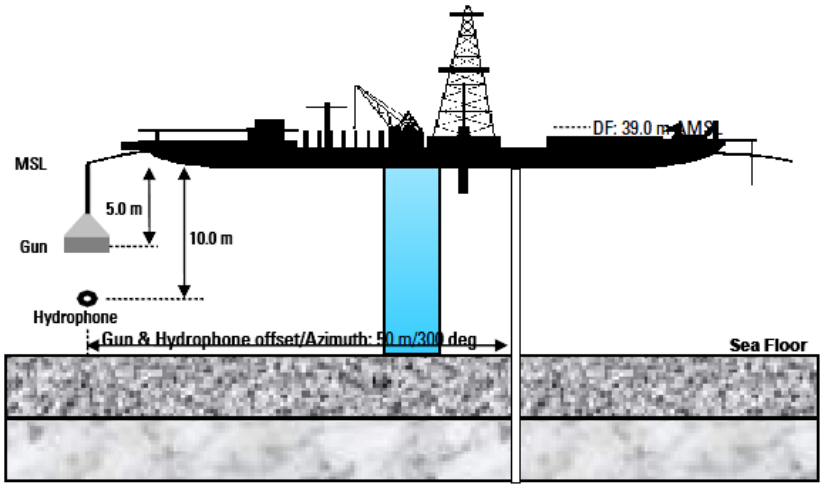

Fig. 4. Schematic representation of design and acquisition of VSP data corresponding to the well in this study (NISOC 2005).

3. VSP DATA PROCESSING AND SHEAR WAVE SPLITTING

3.1 Fast and slow shear wave

First step of shear wave splitting includes determination of fast and slow shear wave slowness for evaluating the possible intervals showing anisotropy. To do this, processing the 3-component near offset VSP data acquired from a deviated well was done. Thus, first-break times were picked on the raw vertical component traces, initial velocity was obtained by the location of the receivers and all traces were filtered with a 10-50 Hz zero-phase bandpass filter to remove high frequency noise. Figure 5 shows the raw *X*- and *Y*-components while Fig. 6 gives the *Z*-components of VSP along with the raw velocity obtained by first break time picking.

Comparing to surface seismic data, the wavefields recorded in VSP data sets are much more complicated due to the downhole location of the receivers. For a *P*-wave source in VSP data, major wave modes present in the VSP

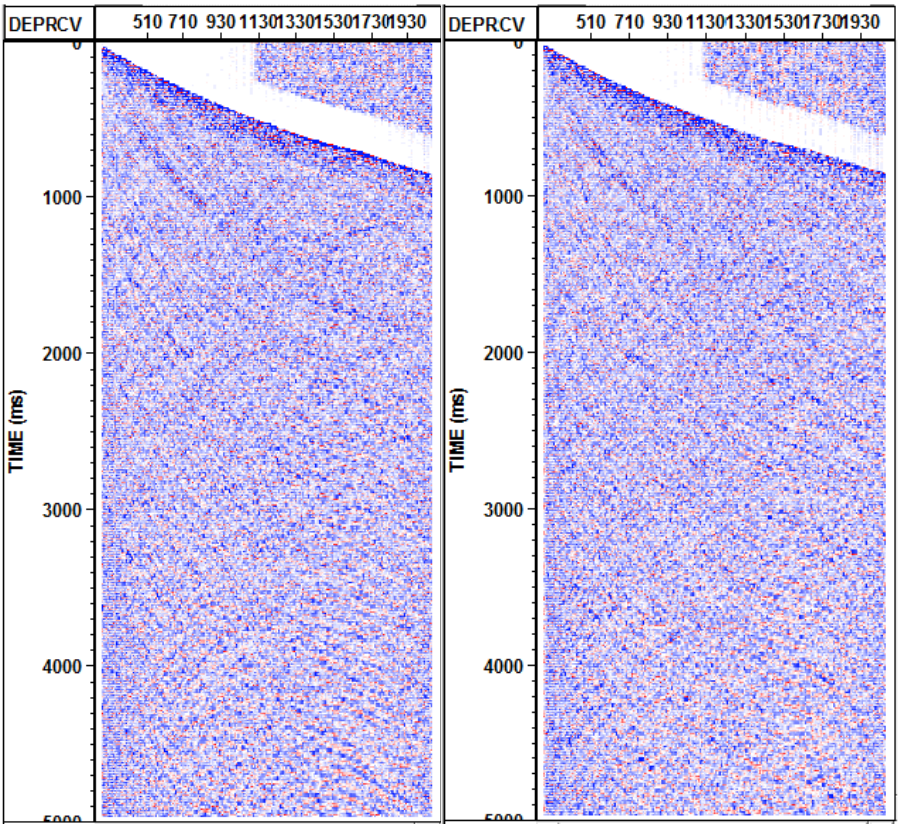

Fig. 5. Raw horizontal components of VSP acquisition in the well under this study: *Y*-component (left) and *X*-component (right).

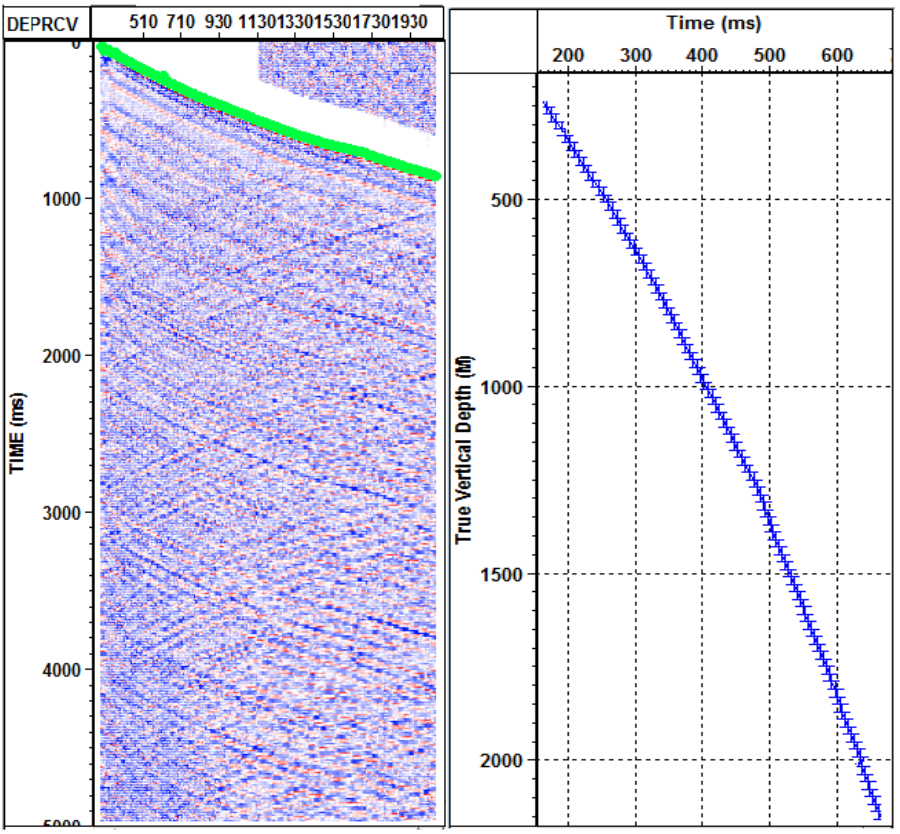

Fig. 6. Raw vertical component (left) with first arrival time picking (*i.e.*, green line) and travel time of first arrival *P*-wave (right).

data include upgoing and downgoing *P*-waves (P_v), downgoing and upgoing shear waves (S_v), and horizontal shear wave (S_h).

The main object of this study was to pick the first arrival time of fast and slow shear waves. Thus, polarization reorientation of the multi-component data was performed using the Hodogram analysis. Hodogram analysis is based on the amplitudes in the short time windows given by the first breaks of 3C data. Its basic principle is to use the amplitude cross-plot of first breaks in an orthogonal coordinate system to find the wavefield polarization angle between two component data (Gulati *et al.* 2004). After polarization analysis of raw *X*- and *Y*-components, there will be two new components known as *H* (horizontal) and *T* (transverse) components containing *P*-waves and *SV*-waves travelling in the vertical plane and S_h wave travel perpendicular to this plane, respectively. Hodogram analysis of *Z* component and *H*

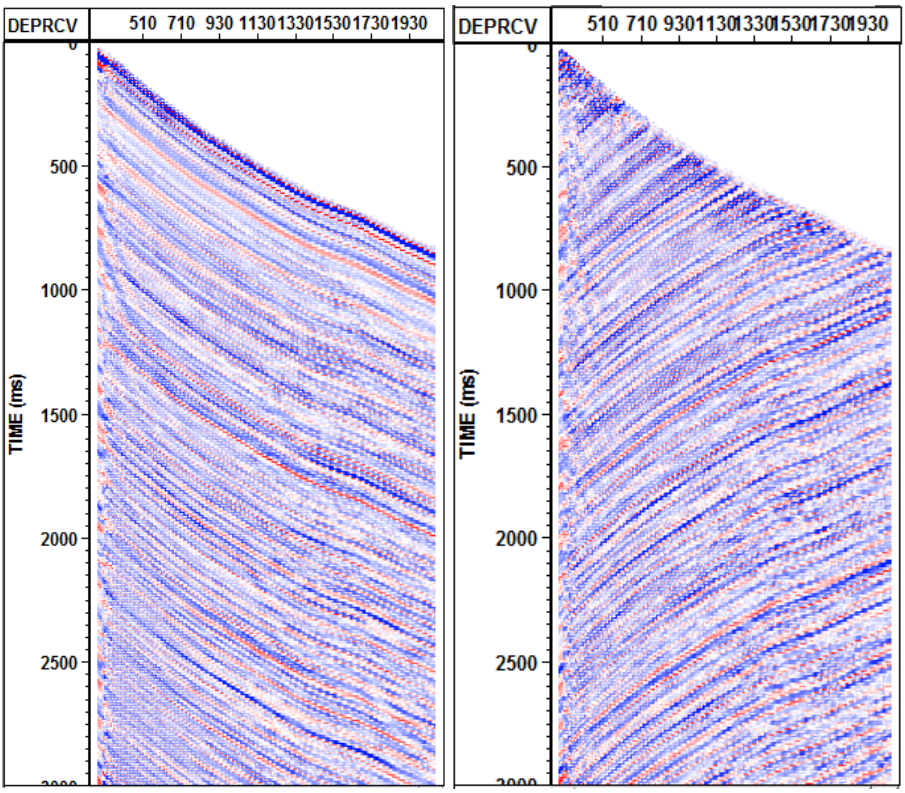

Fig. 7. Downgoing (left) and upgoing (right) components extracted from *V*- and *R*-components.

component yielded two new components called *V* (vertical) and *R* (radial) components. Both of these contain upgoing and downgoing *P*- and *S*-waves. However, intensity of shear wave in *R*-component is much higher than that of the *V*-component. Vertical component mainly contains the *P*-wave. To separate downgoing and upgoing waves, radon transform was used. The F-K filter is the conventional type of filtering space used to discriminate the up-going and downgoing waves. However, the success of F-K filtering depends strongly on the degree to which events are mapped into distinguished regions in the F-K domain. If, for example, many events are present in the data, these events overlap in the F-K domain and their separation is complicated (Theune *et al.* 2006). To circumvent this inherent problem of F-K filtering for coherent noise suppression, radon transform can be used (Nuzzo and Quarta 2004). The radon transform pair is expressed as:

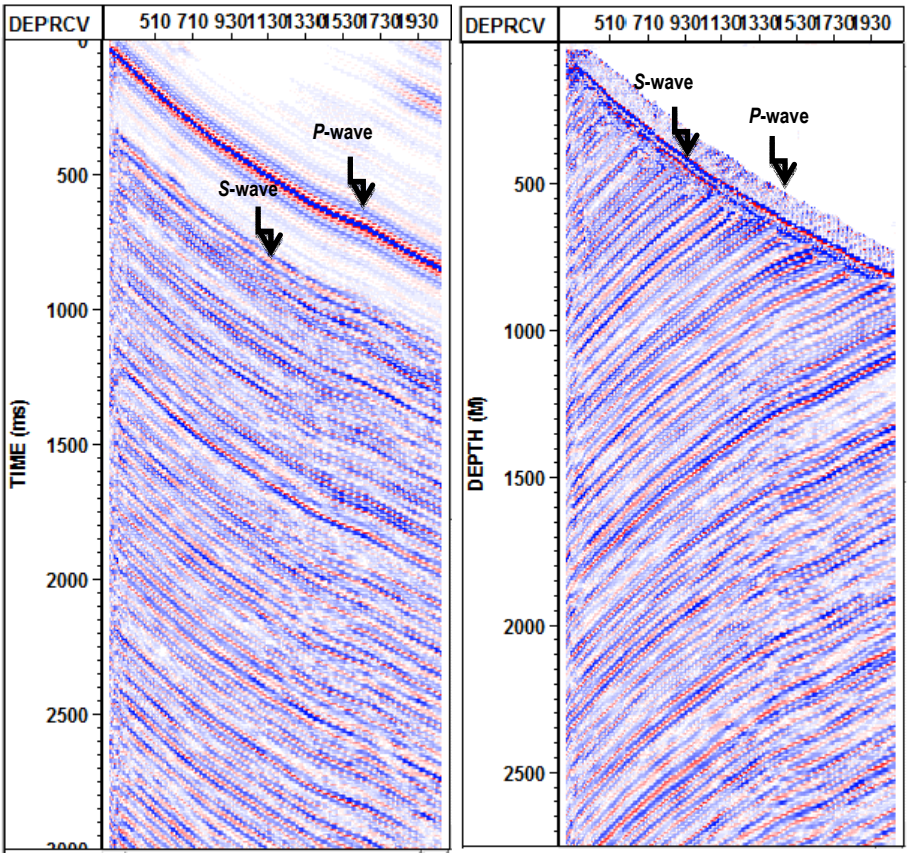

Fig. 8. Downgoing *P*- and *S*-waves (left) and upgoing *P*- and *S*-waves (right) obtained from time variant analysis.

$$\begin{cases} \psi(\omega, p) = \dfrac{|\omega|}{2\pi} \int_{-\infty}^{+\infty} \varphi(\omega, x) e^{i\omega p x} dx \\ \varphi(\omega, x) = \int_{-\infty}^{+\infty} \psi(\omega, p) e^{-i\omega p x} dp \end{cases} \tag{1}$$

In the above equations, ψ and φ are, respectively, wavefield in frequency-slowness and frequency-space domains. Parameter p is slowness, ω is angular frequency, and x is distance.

Applying the radon transform upgoing and downgoing waves were extracted from *V*- and *R*-components, respectively. Figure 7 shows the upgoing and downgoing waves obtained through radon transform filtering.

Before separating the *P*- and *S*-waves, tube wave should be removed from the components. However, due to being marine date acquisition, tube

wave cannot be found in acquired data. To separate upgoing and downgoing *P*- and *S*-waves, in the current paper a new approach known as time-variant analysis was used. This approach uses propagation direction and polarization orientation for various waves at different travel times. In this approach, calculations are done in time-spatial domain rather than frequency or any other domains. Undoubtedly, time and spatial variant propagation and polarization information of the waves will be much more accurate and helpful for wavefield separation. To implement this approach, those steps mentioned earlier including azimuthal corrections and separation of upgoing and downgoing waves should be done. To calculate propagation direction and polarization orientation of the wavefields forward modeling can be simply used. Assuming linear polarization of the wavefields, upgoing P_v- and S_v-waves in vertical and radial components can be reoriented on their own polarization planes. Thus, two polarization planes, one for the upgoing *P*-wave and an-

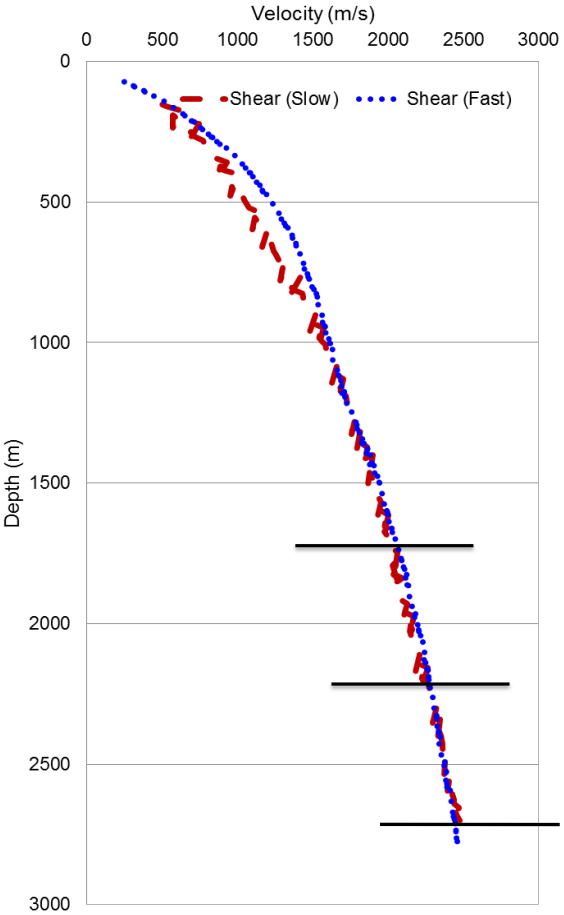

Fig. 9. Fast and slow *S*-wave velocity obtained from VSP data analysis.

other one for the upgoing *S*-wave, will be set up. Downgoing waves in this method are considered to be residual in the two planes which can be removed by radon transform or even F-K filtering. Figure 8 shows the results obtained through utilizing this method for wavefield separation.

As shown in Fig. 8, the methodology used here is able to highlight the first arrival time of the downgoing and upgoing *P*- and *S*-waves. In addition, we still need the horizontal *S*-wave for doing the complete analysis and determining which one of the shear waves is the faster and which one is the slower. According to the number of studies carried out in this area of research, *T* (transverse) component obtained through hodogram analysis of Raw *X*- and *Y*-components contains S_h wave (Liu *et al.* 2012). Thus it is possible to do shear wave splitting analysis. Figure 9 shows the fast and slow shear waves obtained from first arrival time of upgoing S_v and S_h.

As indicated in Fig. 10, difference between the fast and slow shear waves in the interval of 2000 to 2250 m can be attributed to fractured sandstone reservoirs as Burgan A and B reservoirs located in such interval. Velocity difference of shear waves in the interval between 1450 to 2000 m is related to the extensive existence of shale layer in the cap rock of the reservoir. Being sure about the application of VSP data processing in fracture detection, in the next step fracture strike detection is done and discussed in details.

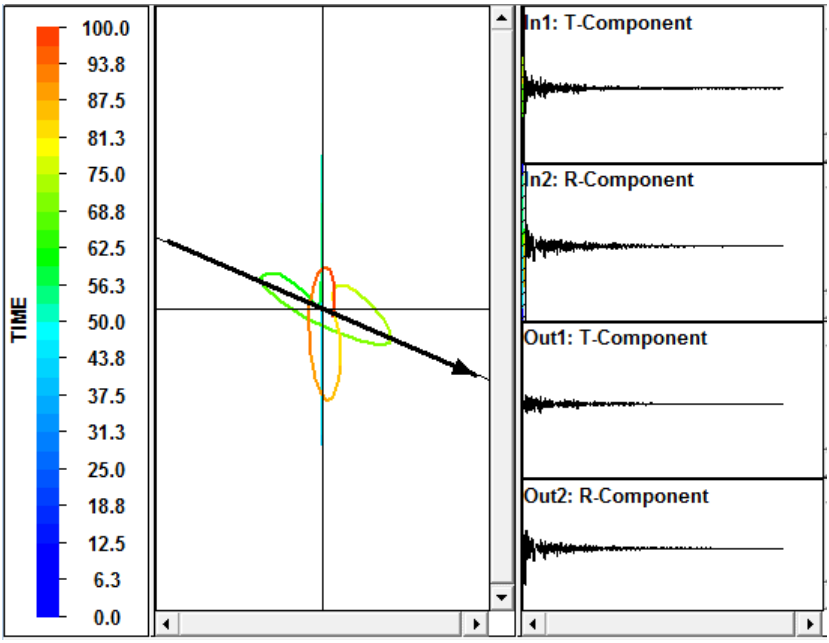

Fig. 10. Hodogram analysis of radial and transverse components before rotation to be in direction of horizontal components.

3.2 Fracture strike detection

Shear-wave splitting (SWS) is a valuable tool based on the observation of shear-wave propagating for characterization of aligned microcracks and fractures. In this method, faster shear wave is polarized parallel to the crack direction and slower one is polarized perpendicular to it (Crampin and Peacock 2005). In this case, polarization direction of the fast shear-wave is parallel to cracks orientation regardless of the initial polarization at the source (Peacock *et al.* 1988). The time delay between the arrival of the faster and the slower shear-waves on the other hand will be proportional to crack density (Hudson 1981, Crampin 1987, Crampin and Lovell 1991) and can be used for crack characterization. These two shear-wave splitting parameters known as polarization direction (φ) and time delay (Δt) are valuable data to estimate subsurface fracture geometry, its density and permeability within fractured reservoirs.

For the purpose of this study, as it was mentioned earlier, wavefield separation was done by a sequence of two two-component rotations, and by radon filters in the common-shot gather domain. Using the VSP data from a *P*-wave source, the difference between the fast and slow shear waves propagating in two different transverse and radial directions can be an indication of possible fracture in subsurface layers. Conventional analysis done for fracture strike direction involves rotation of horizontal component data into the natural coordinate system through the use of standard methods such as Alford rotation (Alford 1986), or the linear transform using hodogram analysis (Li and Crampin 1993). In addition, according to the Long (2010), shear wave splitting analysis for determination of fracture strike can be done by searching for maximum correlation and most linear particle motion between the transverse (T) and radial (R) components. To determine fast shear wave polarization angle φ the two components therefore are interactively rotated until the horizontal particle motion plot shows that fast and slow shear-waves are oriented along the instrument's horizontal components. In this case, there will be a completely linear correlation between the two components containing shear waves. This angle of rotation from the original polarization direction determines φ. Time delay, on the other hand, can be directly measured by the difference between arrival times of two shear waves in various intervals. Figure 10 shows the correlation between the fast and shear wave before the rotation carried out for determination of polarization direction.

As can be seen in Fig. 10, due to anisotropy in subsurface layer which can be due mainly to fractured sandstone reservoirs in the interval highlighted in Fig. 9, fast and slow shear wave particle motion has an elliptical shape. This shape is changed to be in a linear form when these two waves polarized

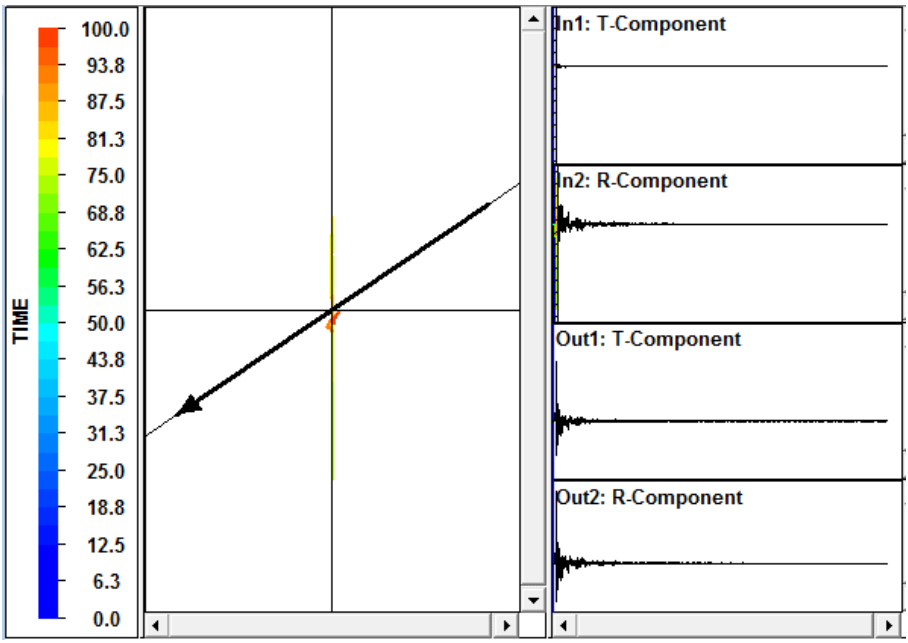

Fig. 11. Hodogram analysis of radial and transverse components after rotation to be in direction of horizontal components with linear particle motion.

in the direction of instrumental horizontal components. This change in particle motions is depicted in Fig. 11.

According to the plot shown in Fig. 11, polarization angle φ of the fast shear wave is approximately 86 degrees. This angle is approved with looking at the signals shown in the right side of Fig. 11 as those signals almost completely match with each other at the output. This polarization angle which corresponds to the strike of fractures can be simply shown in rose diagram by converting the angle to be azimuth. Figure 12 shows the rose diagram plot of fracture strike obtained by determination the polarization angle of fast shear wave.

As shown in Fig. 12, E indicates the direction of horizontal component parallel to *X*-axis whereas N expresses the direction of horizontal component parallel to *Y*-axis. Vertical *Z*-component is perpendicular to the E-N plane. The longest bar in the rose diagram shows the main strike of fractures in subsurface layer in N-E (*i.e.*, *X*-*Y* plane). Considering the polarization angle in *X*-*Y* plane of instrumental components, azimuth of fast shear wave polarization in N-E plane will be N4E. This result has an acceptable match with the fracture orientation obtained from core data analysis in the lab.

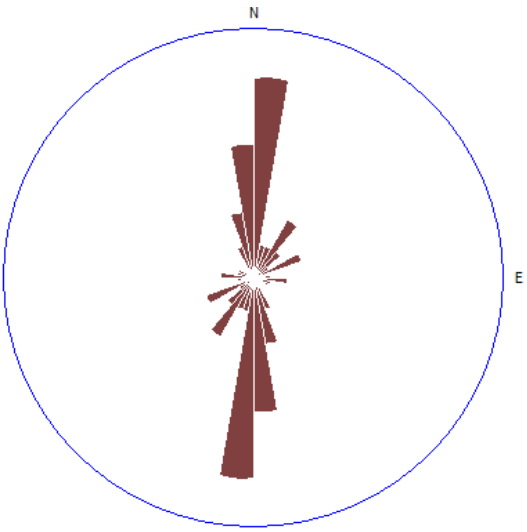

Fig. 12. Rose diagram obtained by converting the angle of maximum polarization into azimuth.

4. FREQUENCY-DEPENDENT ANISOTROPY

Seismic anisotropy is a widely used tool for assessment of fractured rocks and fluid migration in subsurface layer. To do this type of analysis, various medium theories have been proposed which have been found with limited applications due to their theoretical constraints. There are few publication literatures discussing on the frequency-dependent anisotropy, especially in geophysical exploration. This topic, however, has been reported in earthquake literature by Marson-Pidgeon and Savage (1997). They indicated that time-delay decreases as frequency increases. However, it should be noticed that even heterogeneity can produce apparent anisotropy which should not be mistaken with anisotropy induced by fractures or weak planes (Marson-Pidgeon and Savage 1997). Frequency-dependent anisotropy can be evaluated due to scattering of seismic waves in heterogeneous mediums. For example, Werner and Shapiro (1999) have shown that anisotropy will be different in various frequencies. This means that heterogeneous mediums can behave like an anisotropic medium at some frequencies in the case of having certain alignments. However, influence of heterogeneities decreases as the frequency increases and wavelength decreases. This implies that waves with various periods are sensitive to anisotropy of structure at different scale. This means, lower frequency bands measurements tend to smooth small-scale heterogeneities while high-frequency measurements are sensitive to these small-scale changes. In fact, the scale of heterogeneities should be

small enough to cause effective anisotropy rather than scattering (Sato and Fehler 1997). Chesnokov *et al.* (2001) proposed a model addressing the frequency dependent anisotropy in the presence of orientation in heterogeneities medium. They revealed that anisotropy can only be observed when the wavelengths of waves are much greater than the sizes of inhomogeneities.

Another most likely phenomenon causing frequency-dependent anisotropy is fluid flow in fractured rocks. This subject has been studied in the last decades to evaluate velocity dispersion and frequency dependent anisotropy in porous rocks. Bayuk and Chesnokov (1998) were pioneers in assessing the correlation between *P*- and *S*-waves anisotropy in fractured rocks. They concluded that seismic waves can be a useful asset for distinguishing fluid properties of fractured reservoir rocks. Chapman *et al.* (2003) placed aligned fractures in porous media and indicated that fluid flow can occur at grain and fractures scales and hence anisotropy is a frequency-dependent phenomenon. Thomsen (1995) concluded that at seismic frequencies, little dispersion may induce on the waves due to anisotropy. Chapman *et al.* (2003) revealed that frequency dependence may be expected to be observed in the presence of larger scale fractures in the seismic frequency ranges but not in low frequency limit. Tod and Liu (2002) presented a model to describe fluid flow in elliptical cracks and pointed out that fluid flow is not negligible and play significant role in observing frequency-dependent anisotropy. Therefore, the shear wave splitting sensitivity depends mostly on frequency, heterogeneity, and fractures in the background anisotropic structure (Long *et al.* 2008). In the following sections, frequency dependent anisotropy is evaluated and discussed through utilizing a three-component near offset VSP data in the studied well.

4.1 Frequency-dependent anisotropy analysis using 3C-near offset VSP data

To do frequency-dependent anisotropy analysis, hodogram analysis and component rotation were performed after a series of zero-phased band-pass filtering on the transverse (which contains S_h wave) and radial (which contains S_v wave) components aiming to do shear wave splitting for each frequency band. Hence, these components were band pass filtered to have three distinct frequency bands of 0-15, 15-30, and 30-45 Hz. Having these three frequency bands, polarization analysis was carried out to determine polarization angle corresponding to each band. Figure 13 shows the polarization angles obtained through successive rotation of components classified into three frequency bands.

As shown in Fig. 13, except for very low frequency, polarization angles in the reservoir interval are in acceptable agreement with those obtained

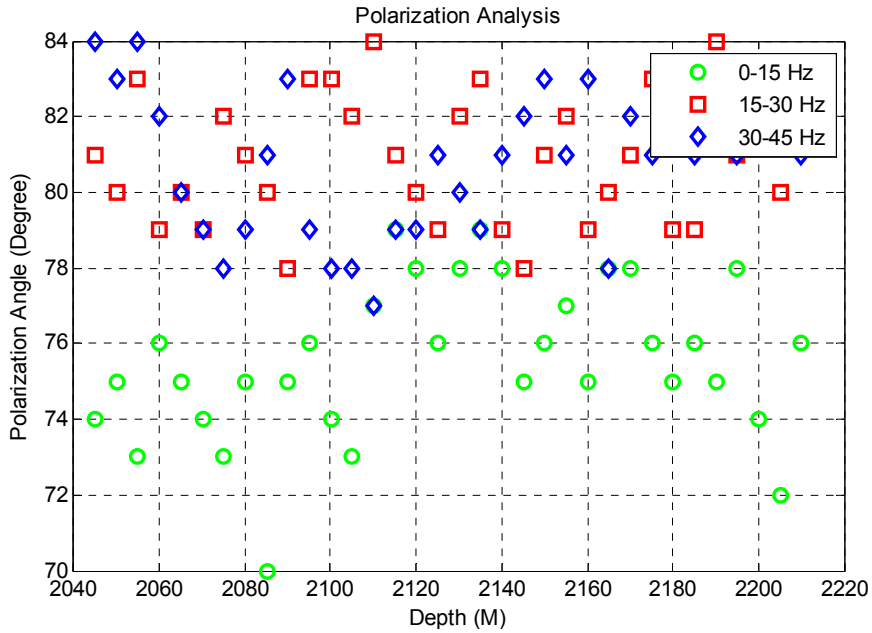

Fig. 13. Polarization angle of fast shear wave splitting.

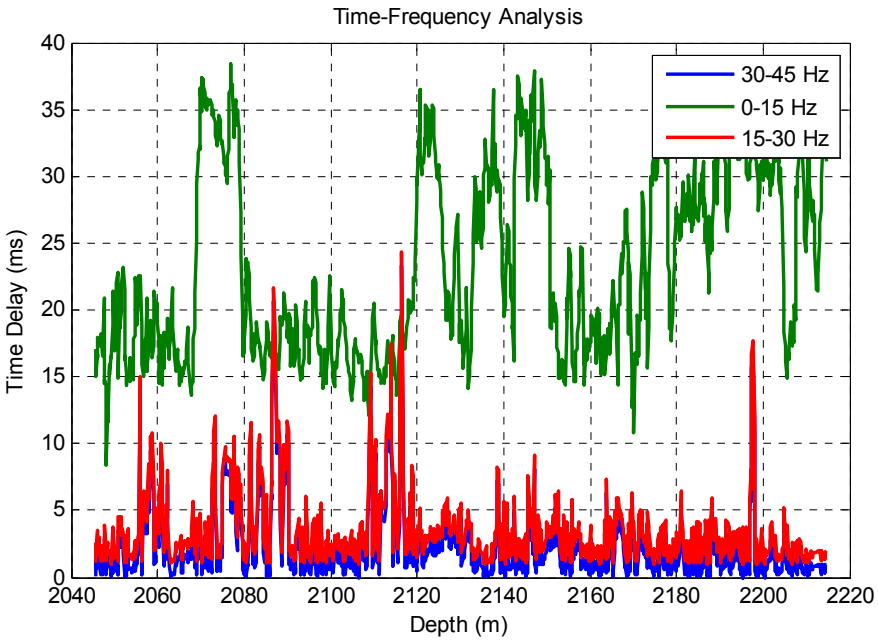

Fig. 14. Variation of time delay between fast and slow shear waves.

from the earlier rotation analysis for determination of fast shear wave polarization direction. Figure 14 shows the variations of time delays between fast and slow shear-waves obtained in different frequency bands.

In Fig. 14, four distinct intervals can be identified as the seismically anisotropic area in high frequency: 2530-2060, 2071-2090, 2112-2118, and 2196-2198 m. In other depth intervals, however, the time delays remain almost constant, implying that these intervals are isotropic in terms of the propagation of waves as there is no further shear-wave splitting observed. In very low frequency, very high time delay is observed which may be attributed to the existence of heterogeneity in the intervals. It should be noticed that layer stripping method will not be necessary to be implemented here as there is no obvious change in polarization with depth, revealing that fracture orientation is not changing with depth at least across the interval between 2040 and 2210 m. As it has been depicted in Fig. 14, time delays of frequency between 15-30 and 30-45 Hz are similar to each other and can clearly show the variation of shear wave splitting in the reservoir interval. In this interval, the shear-wave anisotropy occurs due to the presence of open and aligned vertical fractures, as it was already mentioned. If it is assumed that the magnitude of shear-wave anisotropy (time delays between split shear-waves) is proportional to fracture density, then the highest density of open, fluid-filled fractures is interpreted to be in the interval between 2060 and 2120 m. Figure 15

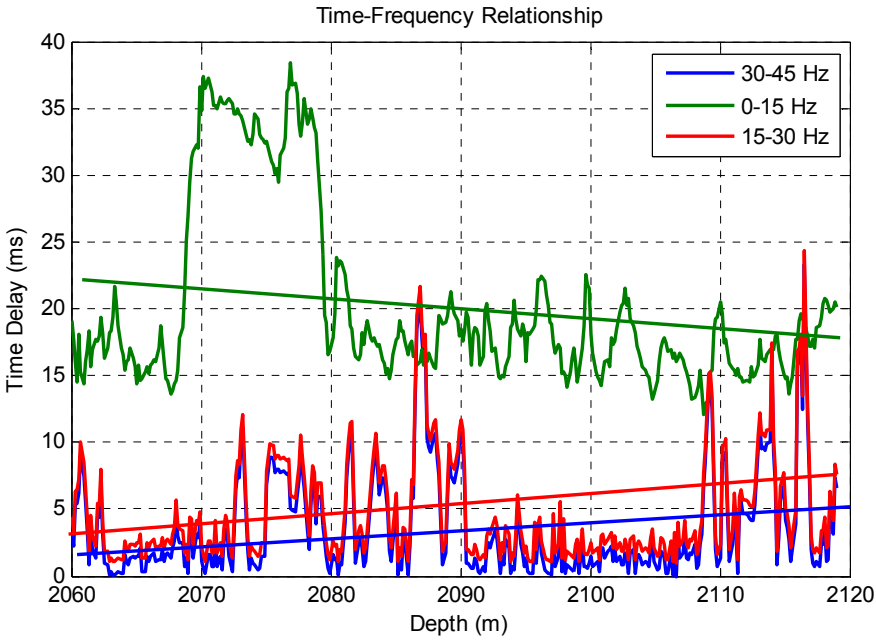

Fig. 15. Time delays across interval with highest density of open, fluid-filled fractures.

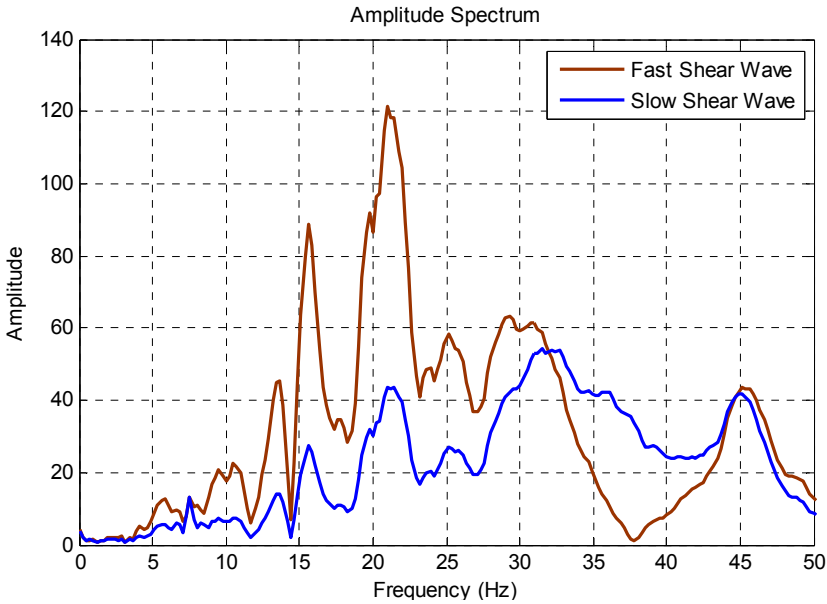

Fig. 16. Amplitude spectral plot of the fast and slow shear wave components.

shows the time delays in the interval with highest density of open and fluid-filled fractures.

As depicted in Fig. 15, time delays linearly increase with depth and decrease as frequency increases. A linear regression was applied to fit the time delay variations with depth for each frequency band. Except for the lowest frequency band (0-15 Hz), at which the variation of amplitude is small, a decrease in the gradient of time delays can be clearly seen. It should be noted that while the model proposed by Tod and Liu (2002) indicated that low frequency may be an important parameter to take into consideration, in this study it was found that it may have application in characterization of medium heterogeneity. It was also concluded that as the frequency increases, anisotropy due to time delay is reduced. Figure 16 shows the amplitude spectral plots of the fast and slow shear wave components.

Having high amplitude energy in fast shear wave component can be due mainly to the processing steps done to separate qP, qS_v, and qS_h. In fact, components' rotation carried out by the hodogram analysis reduces the energy in the T-components and enhances the energy concentrated on R-component. According to the results shown in Fig. 16, one may consider the band-pass filtering technique as one of the factors in observing variation of anisotropy with frequency. It should be noticed that according to the uncertainty principle, it is impossible to have optimal resolution in time and frequency at the same time.

5. DISCUSSION

Seismic anisotropy analysis is one the recent discussions in seismic exploration which essentially deal with characterization of fractured rocks in order to have better understanding of fluid flow migration. Plenty of theories have been proposed in the recent years trying to relate seismic parameters to properties of rock mass. Most of these theories were found applicable but due to their limitations and assumptions, accuracy of the results will be questionable. The important matter which has not yet been considered in most of these medium theories is the relationship of frequency with the existence of fractures in rocks. It should be noticed that in order to discriminate heterogeneity of fractures, which both can be considered as the main reason of seismic anisotropy in different frequencies, frequency analysis should be done carefully as different critical wavelength ranges may reflect different physical mechanisms. This is one of the most significant limitations of current medium theories which have not yet been addressed appropriately. Although attempts were made in this study to show how frequency and seismic anisotropy are relatively inked to each other based on VSP seismic data analyzed in three distinct frequency bands, more studies are still required to be done to address this mater and add these vital parameters into medium theories so as to reduce the misinterpretation of fractures with heterogeneity.

6. CONCLUSIONS

In this paper, shear-wave splitting and frequency analysis was demonstrated using a three component near offset VSP data acquired from a fractured reservoir. Using hodogram analysis of radial and transverse components of the VSP data, fracture orientation across the reservoir layer was estimated. Performing frequency dependent anisotropy, it was shown that there is no apparent relationship between polarization and frequency since spatial distribution of fracture orientation did not change with frequency. Time-delays between fast and slow shear-waves which are proportional to fracture density indicated that frequency increases as the time delay increases. At the same time, anisotropy observed due to time delays decreases as the frequency increases. The results obtained in this paper can be a supplementary study for the other researches performed in this field.

References

Alford, R.M. (1986), Shear data in the presence of azimuthal anisotropy: Dilley, Texas. **In:** *56th SEG Annual Meeting, 2-6 November 1986, Houston, USA*, Society of Exploration Geophysicists, Expanded abstracts, SEG-1986-0476, 476-479.

Bayuk, I.O., and E.M. Chesnokov (1998), Correlation between elastic and transport properties of porous cracked anisotropic media, *Phys. Chem. Earth* **23**, 3, 361-366, DOI: 10.1016/S0079-1946(98)00038-X.

Chapman, M., S. Maultzsch, E. Liu, and X.Y. Li (2003), The effect of fluid saturation in an anisotropic multi-scale equant porosity model, *J. Appl. Geophys*. **54**, 3-4, 191-202, DOI: 10.1016/j.jappgeo.2003.01.003.

Chesnokov, E.M., Y.A. Kukharenko, and P.Y. Kukharenko (1998), Frequency-dependence of physical parameters of microinhomogeneous media: space statistics, *Rev. Inst. Fr. Petrol.* **53**, 5, 729-734, DOI: 10.2516/ogst:1998065.

Chesnokov, E.M., J.H. Queen, A.A. Vichorev, H.B. Lynn, J.M. Hooper, I.O. Bayuk, J.A. Castagna, and B. Roy (2001), Frequency dependent anisotropy. **In:** *71st SEG Annual Meeting, 9-14 September 2001, San Antonio, USA*, Society of Exploration Geophysicists, Expanded abstracts, 2120-2123, DOI: 10.1190/1.1816569.

Crampin, S. (1985), Evaluation of anisotropy by shear-wave splitting, *Geophysics* **50**, 1, 142-152, DOI: 10.1190/1.1441824.

Crampin, S. (1987), Geological and industrial implications of extensive-dilatancy anisotropy, *Nature* **328**, 6130, 491-496, DOI: 10.1038/328491a0.

Crampin, S., and J.H. Lovell (1991), A decade of shear-wave splitting in the Earth's crust: what does it mean? What use can we make of it? And what should we do next? *Geophys. J. Int.* **107**, 3, 387-407, DOI: 10.1111/j.1365-246X.1991.tb01401.x.

Crampin, S., and S. Peacock (2005), A review of shear-wave splitting in the compliant crack-critical anisotropic Earth, *Wave Motion* **41** 1, 59-77, DOI: 10.1016/j.wavemoti.2004.05.006.

Gulati, J.S., R.R. Stewart, and J.M. Parkin (2004), Analyzing three-component 3D vertical seismic profiling data, *Geophysics* **69**, 2, 386-392, DOI: 10.1190/1.1707057.

Hudson, J.A. (1981), Wave speeds and attenuation of elastic waves in material containing cracks, *Geophys. J. Int.* **64**, 1, 133-150, DOI: 10.1111/j.1365-246X.1981.tb02662.x.

Hudson, J.A., E. Liu, and S. Crampin (1996), The mechanical properties of materials with interconnected cracks and pores, *Geophys. J. Int*. **124**, 1, 105-112, DOI: 10.1111/j.1365-246X.1996.tb06355.x.

Hudson, J.A., T. Pointer, and E. Liu (2001), Effective-medium theories for fluid-saturated materials with aligned cracks, *Geophys. Prospect*. **49**, 5, 509-522, DOI: 10.1046/j.1365-2478.2001.00272.x.

Li, X.Y., and S. Crampin (1993), Linear-transform techniques for processing shear-waves anisotropy in four-component seismic data, *Geophysics* **58**, 2, 240-256, DOI: 10.1190/1.1443409.

Li, X.Y., Y.J. Liu, E. Liu, F. Shen, L. Qi, and Q. Shouli (2003), Fracture detection using land 3D seismic data from the Yellow River Delta, China, *The Leading Edge* **22**, 7, 680-683, DOI: 10.1190/1.1599696.

Liu, E., J.A. Hudson, and T. Pointer (2000), Equivalent medium representation of fractured rock, *J. Geophys. Res.* **105**, B2, 2981-3000, DOI: 10.1029/1999JB900306.

Liu, E., J.H. Queen, X.Y. Li, M. Chapman, S. Maultzsch, H.B. Lynn, and E.M. Chesnokov (2003), Observation and analysis of frequency-dependent anisotropy from a multicomponent VSP at Bluebell-Altamont Field, Utah, *J. Appl. Geophys.* **54**, 3-4, 319-333, DOI: 10.1016/j.jappgeo.2003.01.004.

Liu, J., X. Zeng, J. Xia, and M. Mao (2012), The separation of P- and S-wave components from three-component crosswell seismic data, *J. Appl. Geophys.* **82**, 163-170, DOI: 10.1016/j.jappgeo.2012.03.007.

Long, M.D. (2010), Frequency-dependent shear wave splitting and heterogeneous anisotropic structure beneath the Gulf of California region, *Phys. Earth Planet. In*. **182**, 1-2, 59-72, DOI: 10.1016/j.pepi.2010.06.005.

Long, M.D., M.V. de Hoop, and R.D. van der Hilst (2008), Wave-equation shear wave splitting tomography, *Geophys. J. Int.* **172**, 1, 311-330, DOI: 10.1111/j.1365-246X.2007.03632.x.

Lynn, H.B., K.M. Simon, C.R. Bates, M. Layman, R. Schneider, and M. Jones (1995), Use of anisotropy in P-wave and S-wave data for fracture characterization in a naturally fractured gas reservoir, *The Leading Edge* **14**, 8, 887-893, DOI: 10.1190/1.1437179.

Lynn, H.B., K.M. Simon, and C.R. Bates (1996), Correlation between P-wave AVOA and S-wave traveltime anisotropy in a naturally fractured gas reservoir, *The Leading Edge* **15**, 8, 931-935, DOI: 10.1190/1.1437394.

Lynn, H.B., W.E. Beckham, K.M. Simon, C.R. Bates, M. Layman, and M. Jones (1999), P-wave and S-wave azimuthal anisotropy at a naturally fractured gas reservoir, Bluebell-Altamont Field, Utah, *Geophysics* **64**, 4, 1312-1328, DOI: 10.1190/1.1444636.

MacLeod, M.K., R.A. Hanson, M.J. Hadley, K.J. Reynolds, D. Lumley, S. McHugo, and A. Probert (1999), The Alba Field OBC seismic survey. **In:** *6th Int. Congress of Brazilian Geophysical Society*, Extended abstracts, 6-25.

Magnitsky, V.A., and E.M. Chesnokov (1986), Geophysics of anisotropic media: state of art, *Izv. – Phys. Solid Earth* **22**, 11, 867-872.

Marson-Pidgeon, K., and M.K. Savage (1997), Frequency-dependent anisotropy in Wellington, New Zealand, *Geophys. Res. Lett*. **24**, 24, 3297-3300, DOI: 10.1029/97GL03274.

NISOC (2005), NISOC R&D Solutions Project #1, casing collapse (well integrity); Phase 1 – concept and feasibility study, National Iranian South Oil Company, Ahwaz, Iran.

Nuzzo, L., and T. Quarta (2004), Improvement in GPR coherent noise attenuation using τ–p and wavelet transforms, *Geophysics* **69**, 3, 789-802, DOI: 10.1190/1.1759465.

Parra, J.O. (2000), Poroelastic model to relate seismic wave attenuation and dispersion to permeability anisotropy, *Geophysics* **65**, 1, 202-210, DOI: 10.1190/1.1444711.

Peacock, S., S. Crampin, D.C. Booth, and J.B. Fletcher (1988), Shear wave splitting in the Anza seismic gap, southern California: temporal variations as possible precursors, *J. Geophys. Res.* **93**, B4, 3339-3356, DOI: 10.1029/JB093iB04p03339.

Pointer, T., E. Liu, and J.A. Hudson (2000), Seismic wave propagation in cracked porous media, *Geophys. J. Int.* **142**, 1, 199-231, DOI: 10.1046/j.1365-246x.2000.00157.x.

Qian, Z., X. Li, and M. Chapman (2008), Fracture characterization with azimuthal attribute analysis of P-S wave data: Modelling and application. **In:** *70th EAGE Conference and Exhibition incorporating SPE EUROPEC 2008*, Extended abstracts, DOI: 10.3997/2214-4609.20148062.

Sato, H., and M.C. Fehler (1997), *Seismic Wave Propagation and Scattering in the Heterogeneous Earth*, Springer, Berlin, DOI: 10.1007/978-3-540-89623-4.

Theune, U., M.D. Sacchi, and D.R. Schmitt (2006), Least-squares local Radon transforms for dip-dependent GPR image decomposition, *J. Appl. Geophys*. **59**, 3, 224-235, DOI: 10.1016/j.jappgeo.2005.10.003.

Thomsen, L. (1995), Elastic anisotropy due to aligned cracks in porous rock, *Geophys. Prospect.* **43**, 6, 805-829, DOI: 10.1111/j.1365-2478.1995.tb00282.x.

Thomsen, L.A., O.I. Barkved, B. Haggard., J.H. Kommedal, and B. Rosland (1997), Converted-wave imaging of Valhall reservoir. **In:** *59th EAGE Conference and Exhibition*, Extended abstracts, B048.

Tod, S.R., and E. Liu (2002), Frequency-dependent anisotropy due to fluid flow in bed limited cracks, *Geophys. Res. Lett.* **29**, 15, 1749, DOI: 10.1029/2002GL015369.

Tsvankin, I. (1997), Reflection moveout and parameter estimation for horizontal transverse isotropy, *Geophysics* **62**, 2, 614-629, DOI: 10.1190/1.1444170.

Vetri, L., E. Loinger, J. Gaiser, A. Grandi, and H. Lynn (2003), 3D/4C Emilio: Azimuth processing and anisotropy analysis in a fractured carbonate reservoir, *The Leading Edge* **22**, 7, 675-679, DOI: 10.1190/1.1599695.

Werner, U., and S.A. Shapiro (1999), Frequency-dependent shear-wave splitting in thinly layered media with intrinsic anisotropy, *Geophysics* **64**, 2, 604-608, DOI: 10.1190/1.1444567.

Zhu, X., P. Valasek, B. Roy, S. Shaw, J. Howell, S. Whitney, N.D. Whitmore, and P. Anno (2008), Recent applications of turning-ray tomography, *Geophysics* **73**, 5, VE243-VE254, DOI: 10.1190/1.2957894.

Received 19 April 2013
Received in revised form 9 June 2014
Accepted 9 December 2014